MICROWAVE IMAGING ON METAL OBJECTS

FINAL REPORT

DR. C. L. TOLLIVER

PRAIRIE VIEW A&M UNIVERSITY
PRAIRIE VIEW, TEXAS

APRIL 22, 1998

PREPARED FOR
NASA-LYNDON B.JOHNSON SPACE CENTER
COOPERATIVE AGREEMENT NO. NCC9-40
PROJECT PERIOD: 1995 - 1998

1. *September 1 ~ October 30: Working on SVD method*

We have used Maximum Entropy Method in microwave image reconstruction, but it failed. We also tried Singular Value Decomposition, we didn't get good simulation results. We continue to work on SVD and get some good results.

1) The Algorithm:

Let's consider a set of linear algebraic equations looks like this:

$$\begin{aligned} a_{11}x_1 + a_{12}x_2 + a_{13}x_3 + \ldots + a_{1N}x_N &= b_1 \\ a_{21}x_1 + a_{22}x_2 + a_{23}x_3 + \ldots + a_{2N}x_N &= b_2 \\ a_{31}x_1 + a_{32}x_2 + a_{33}x_3 + \ldots + a_{3N}x_N &= b_2 \\ \ldots \quad \ldots \quad \ldots & \\ a_{M1}x_1 + a_{M2}x_2 + a_{M3}x_3 + \ldots + a_{MN}x_N &= b_M \end{aligned} \tag{1}$$

Here the N unknowns x_j, j = 1, 2, ... , N are related by M equations. The coefficients a_{ij} with i= 1, 2, ... , M and j =1, 2, ... , N are known numbers, as are the right-hand side quantities b_i, ii = 1, 2, ... , M.

Its matrix form can be written as:

$$\mathbf{A} \cdot \mathbf{x} = \mathbf{b} \tag{2}$$

For solution of the above matrix equation for an unknown vector **x**, we can calculate the matrix $\mathbf{A}^{-1}$ which is the matrix inverse of a square matrix **A**, i.e., $\mathbf{A} \cdot \mathbf{A}^{-1} = \mathbf{A}^{-1} \cdot \mathbf{A} = \mathbf{I}$, where **I** is the identity matrix (all zeros except for ones on the diagonal).

For inversion a matrix, we can use Gauss-Jordan elimination or LU decomposition. But in many cases dealing with sets of equations or matrices that are either singular or else numerically very close to singular, they fail to give satisfactory results. A powerful set of techniques to solve the problem is known as singular value decomposition, or SVD.

Singular value decomposition (SVD) is based on the following theorem of linear algebra: Any M × N matrix **A** whose number of rows M is greater that or equal to its number of columns N, can be written as the product of an M × N column-orthogonal

matrix **U**, an N × N diagonal matrix **W** with positive or zero elements (the singular values), and the transpose of an N × N orthogonal matrix **V**. The various shapes of these matrices will be made clearer by the following tableau:

$$\begin{bmatrix} \\ \mathbf{A} \\ \\ \end{bmatrix} = \begin{bmatrix} \\ \mathbf{U} \\ \\ \end{bmatrix} \cdot \begin{bmatrix} w_1 & & & \\ & w_2 & & \\ & & \cdots & \\ & & & w_N \end{bmatrix} \cdot \begin{bmatrix} \\ \mathbf{V}^T \\ \\ \end{bmatrix} \qquad (3)$$

The matrices **U** and **V** are each orthogonal in the sense that their columns are orthonormal,

$$\sum_{i=1}^{M} U_{ik} U_{in} = \delta_{kn} \qquad 1 \le k \le N$$

$$1 \le n \le N \qquad (4)$$

$$\sum_{i=1}^{M} V_{jk} V_{jn} = \delta_{kn} \qquad 1 \le k \le N$$

$$1 \le n \le N \qquad (5)$$

or as a tableau.

$$\begin{bmatrix} \\ \mathbf{U}^T \\ \\ \end{bmatrix} \cdot \begin{bmatrix} \\ \mathbf{U} \\ \\ \end{bmatrix} = \begin{bmatrix} \\ \mathbf{V}^T \\ \\ \end{bmatrix} \cdot \begin{bmatrix} \\ \mathbf{V} \\ \\ \end{bmatrix} = \begin{bmatrix} \\ \mathbf{1} \\ \\ \end{bmatrix}$$

SVD will construct matrix **U**, **V**, and **W**. Then we can get the inverse of **A**:

$$\mathbf{A}^{-1} = \mathbf{V} \cdot \left[\mathrm{diag}(1/w_j)\right] \cdot \mathbf{U}^T \qquad (6)$$

and calculate the unknown vector **x** as:

$$\mathbf{x} = \mathbf{V} \cdot \left[\mathrm{diag}(1/w_j)\right] \cdot (\mathbf{U}^T \cdot \mathbf{b}) \qquad (7)$$

2) Microwave Imaging:

In microwave imaging, the scattered fields can be expressed by the induced current distribution using a non-linear integral equation here.

$$\mathbf{E} = -j\omega\mu \iiint_{(v)} \mathbf{G}(\mathbf{x}, \mathbf{x}') \cdot \mathbf{J}(\mathbf{x}') d^3\mathbf{x}' \tag{8}$$

where $\mathbf{G}$ is the dyadic Green's function which can be expressed as:

$$\mathbf{G}(\mathbf{x}, \mathbf{x}') = \left(\mathbf{I} - \frac{1}{k^2} \mathbf{grad}_x \left(\mathbf{grad}_{x'} \right) \right) \Phi(\mathbf{x}, \mathbf{x}') \tag{9}$$

and $$\Phi(\mathbf{r}) = \Phi(\mathbf{x}, \mathbf{x}') = \frac{e^{-jkr}}{4\pi r}$$

and $r = |\mathbf{x} - \mathbf{x}'| = \left[(x-\xi)^2 + (y-\eta)^2 + (z-\zeta)^2 \right]^{1/2}$, we have

$$\mathbf{E} = -\frac{j\omega\mu_0}{4\pi} \left\{ \iint \left(1 - \frac{jkr+1}{k^2r^2} \right) \frac{\mathbf{J}(\mathbf{r}') e^{-jkr}}{r} ds' + \iint \frac{\mathbf{r}\left(-k^2r^2 + j3kr + 3\right)}{k^2 r^5} \left[J_x \cdot (x-x') + J_y \cdot (y-y') + J_z \cdot (z-z') \right] e^{-jkr} ds' \right\} \tag{10}$$

with $$r = \sqrt{(x-\xi)^2 + (y-\eta)^2 + (z-\zeta)^2}$$

and $$\mathbf{r} = (x-\xi)\mathbf{e}_x + (y-\eta)\mathbf{e}_y + (z-\zeta)\mathbf{e}_z$$

In order to use SVD, we can express the equation (10) into matrix form.

$$\begin{bmatrix} E_x \\ E_y \\ E_z \end{bmatrix} = \begin{bmatrix} B_{11} & B_{12} & B_{13} \\ B_{21} & B_{22} & B_{23} \\ B_{31} & B_{32} & B_{33} \end{bmatrix} \cdot \begin{bmatrix} J_x \\ J_y \\ J_z \end{bmatrix} \tag{11}$$

With (11), we can program on SVD to re microwave image.

3) Computer simulation and results

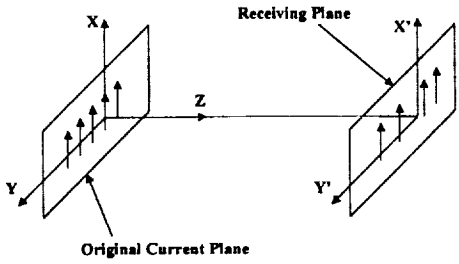

Figure 1 Current and receiving plane

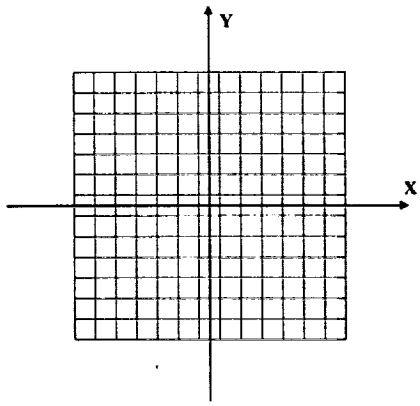

Figure 2 Elements on the current plane

Considering a two-dimensional object situated on the plane XOY (Figure 1) , the induced current is distributed on this plane. The receiving surface (the surface where the scattered field is calculated) may be a plane parallel to the object plane with distance r. Or it may be the surface of a spherical cap with the radius r.

In our calculation, the object plane can be divided into I × I square elements as shown in Figure 2. Similarly, the receiving surface can also be divided into M × N elements according to the requirement of our calculation.

Figure 3 is the computer flow chart for SVD.

Using SVD method to reconstruct image under several conditions. The attached are the simulation results.

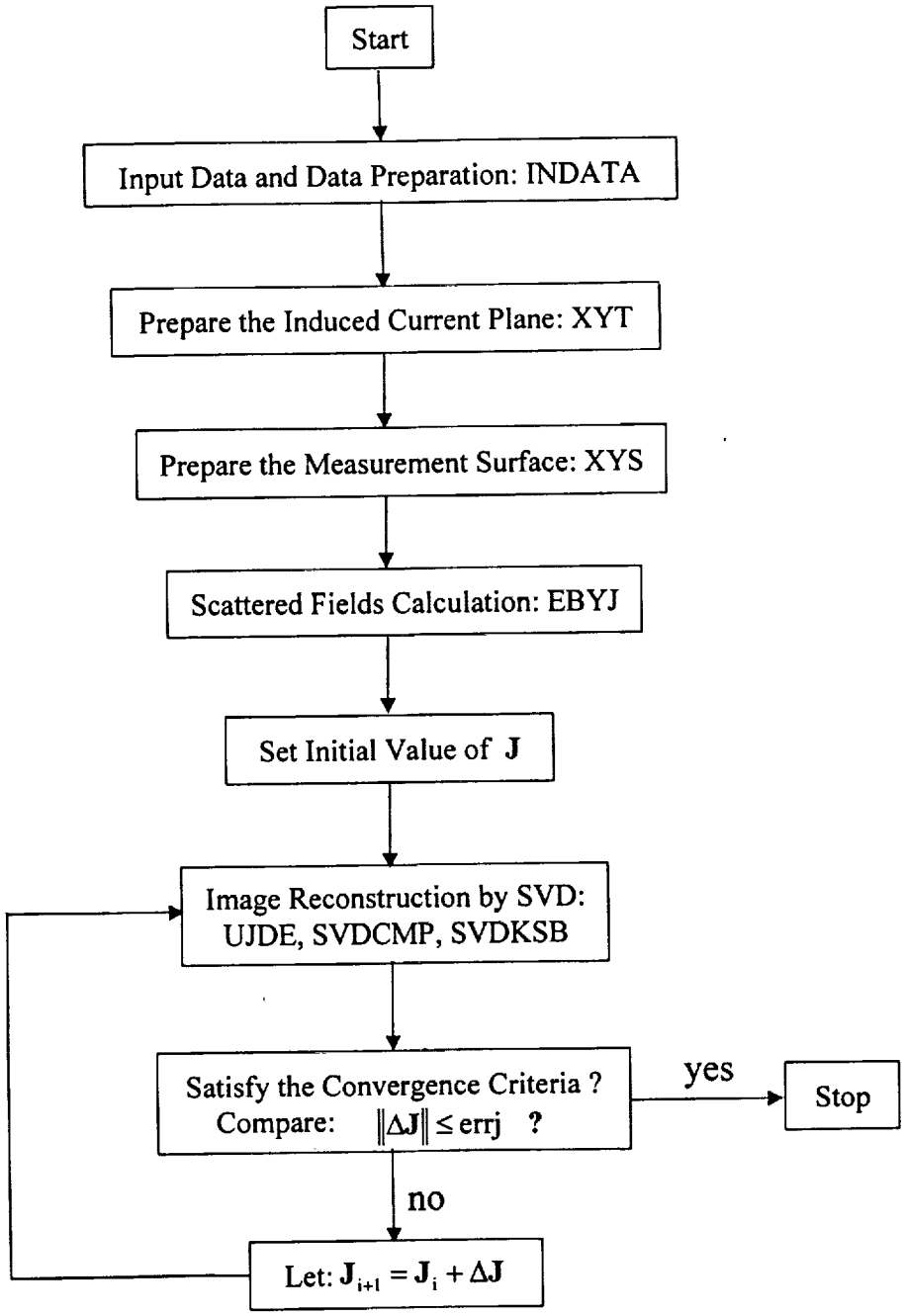

Figure 3 Image Reconstruction by SVD

By the middle of October, we've got some good reconstruction results of microwave image. Still in some cases, the results are not satisfied. The problem lies to the limited data of measurement surface which doesn't contain enough information for image reconstruction. We tried to get more measured points. But this will need large continue computer memory when we solved the inverse problem with SVD. And the computer resource is limited. We can not do like this.

In SVD, we want to solve the ΔJ by the following equation:

$$E_g - E_0 = \Delta E = B \cdot \Delta J \qquad (12)$$

In the program, we use two-dimension array b(n, n) to express the matrix $B_{N\times N}$. If n is too big, the program doesn't work due to lack of enough memory. So we try to separate the array b(n, n) into n arrays of one-dimension . That is b1(1:n). But this method doesn't work because ΔJ and ΔE are all related to the whole array b(n, n). And in Fortran, there is no pointer which can do the address operations. This method failed.

2. *November 1 ~ November 30: working on Conjugate Gradient Method (CGM)*

We have worked on this method before. But it didn't work well. We modified the program and debugged it. Still it can not go to convergence. We found that we separated the real part and imaginary part away during our calculation. And CGM is also written for the real number calculation. So we started to modify our program to be able to do the complex number calculation in the front part. Then we will convert the complex calculation into real number calculation for CGM. This work has not finished.

3. *December ~ April: write and defend the thesis*

In this period, the graduate student arrange the computer simulation data, write the thesis. Finally, she will defend the thesis.

P. S. The computer simulation results. (pp. 7– 36)

Simulation Results

1. Images with Field Measured at Planar Surface

When the scattered field is measured at a plane which is parallel to the object plane, the images recovered as shown in Figure 1.1 – Figure 1.2 with two different kind of original induced current distribution.

The original induced current plane is divided into M × M square elements. The area for each element is $S_J = 0.1\text{m} \times 0.1\text{m}$. This plane is simplified as the **J** plane.

The receiving plane where the scattered field is measured is divided into N1 × N2 square elements. The area for each element is $S_E = 0.1\text{m} \times 0.1\text{m}$. This plane is simplified as the **E** plane.

We can see from these graphs that when the initially guessed **J** is totally different from the original current distribution, the images recovered are not good as those whose initially guessed **J** have the similar distribution with the original ones. An important factor to this is that when the receiving surface is a plane, the measured data contain not enough information to reconstruct the images.

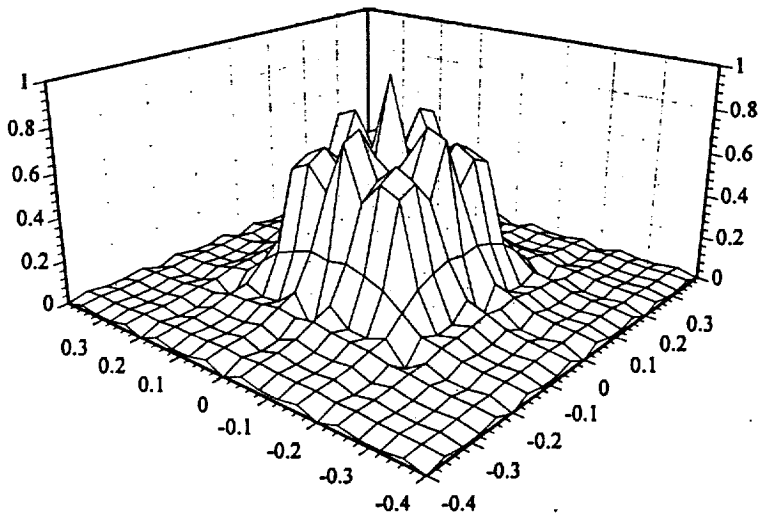

Figure 1.1 (a) The original current **J** with rectangular distribution
9 × 9 square elements in **J** plane
6 × 9 square elements in **E** plane

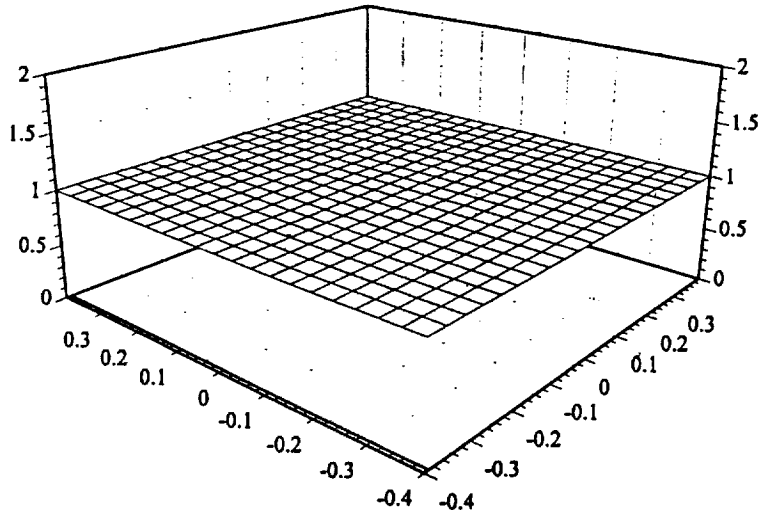

(b) Guessed **J** distribution

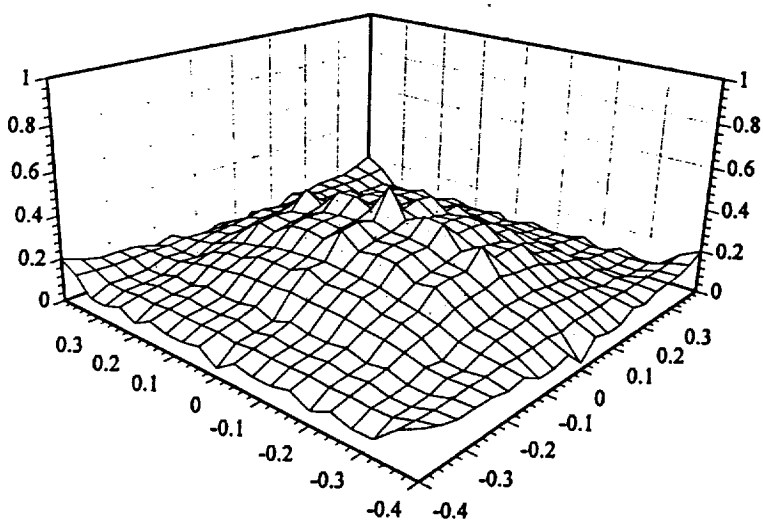

(c) Current image with f = 0.1GHz, z = 1λ

Figure 1.1 Continued

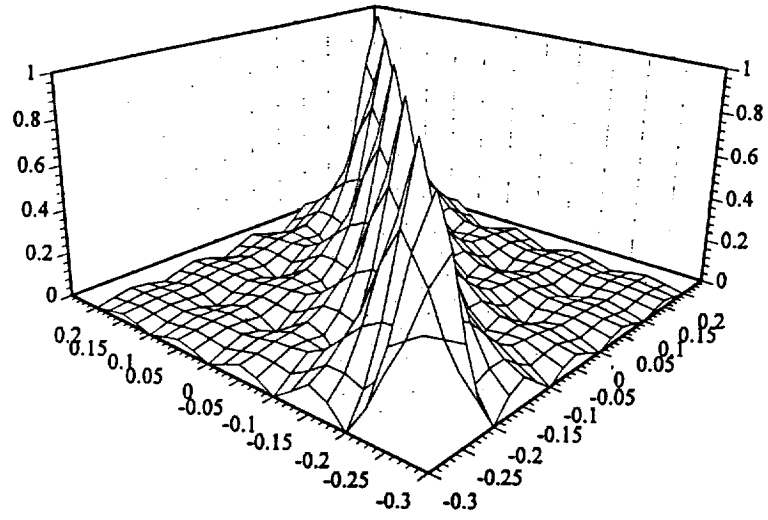

Figure 1.2 (a) The original current **J** with rectangular distribution
6 × 6 square elements in **J** plane
4 × 6 square elements in **E** plane

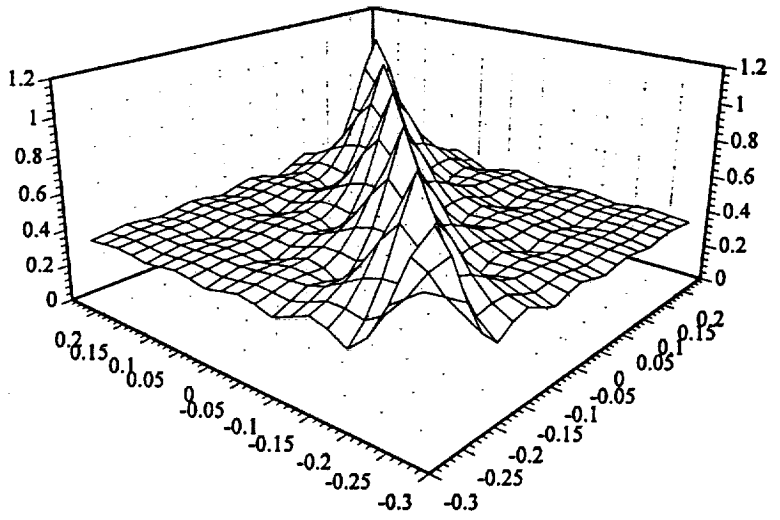

(b) Guessed **J** distribution

Figure 1.2 Continued

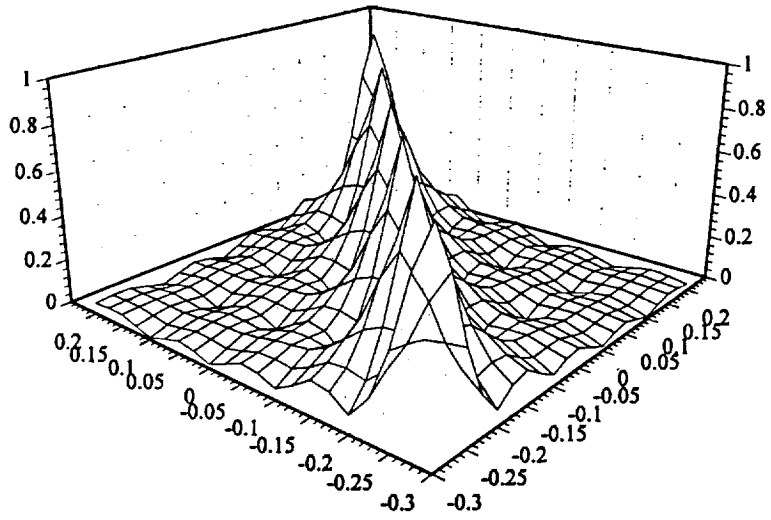

(c) Current image with f = 0.1GHz, z = 1λ
With guessed **J** in (b)

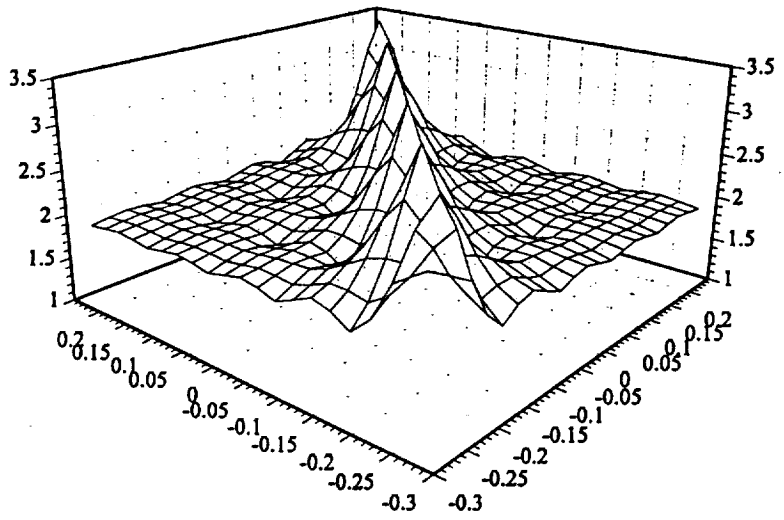

(d) Guess **J** distribution

Figure 1.2 Continued

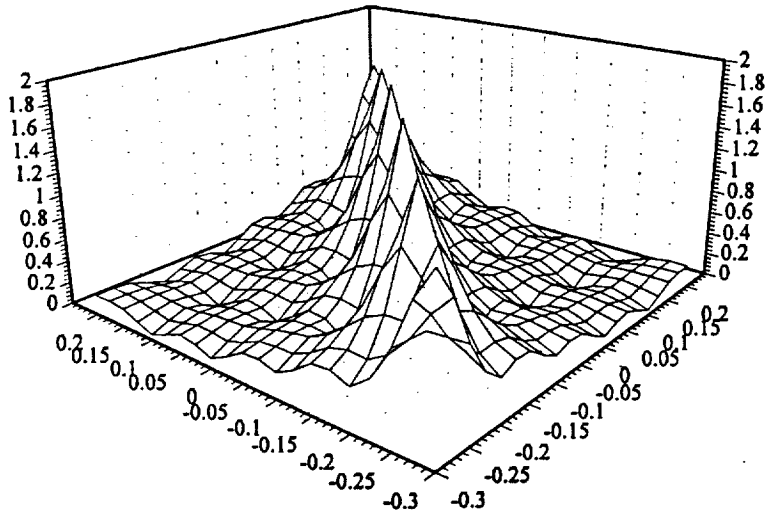

(e) Current image with f = 0.1GHz, z = 1λ
With guessed **J** in (d)

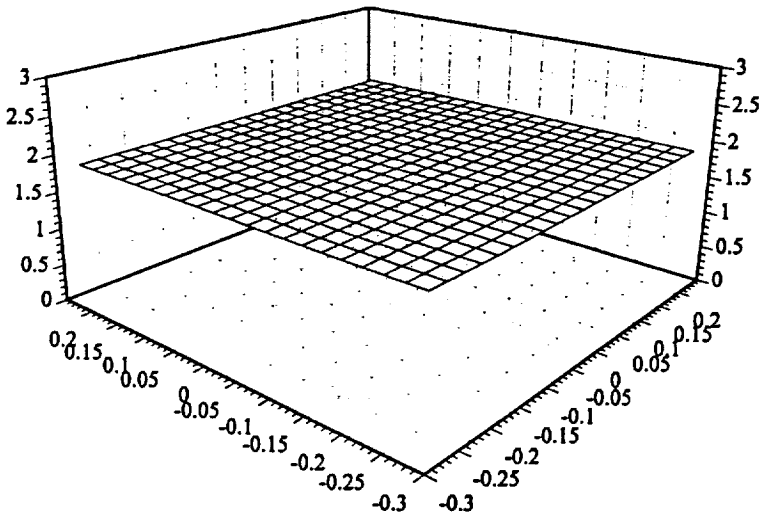

(f) Guessed **J** distribution

Figure 1.2 Continued

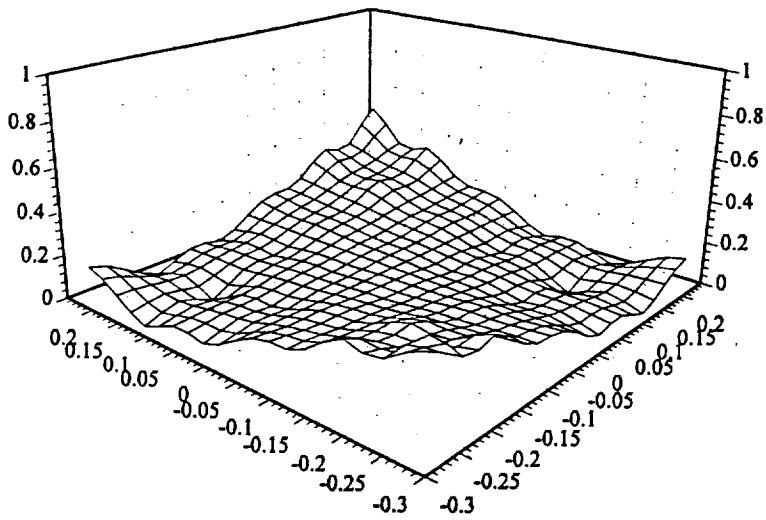

(g) Current image with f = 0.1GHz, z = 1λ
With guessed **J** in (f)

Figure 1.2 Continued

2. Images with Field Measured at Spherical Surface

As we can see from the graphs in section 1 , the images recovered are not ideal. We change the receiving surface from the plane into a spherical cap surface with the radius is r as shown in Figure 2.1 With the spherical cap receiving surface, measured points with different coordination system parameters (r, θ, φ) contain more useful information to recover the images than those of receiving plane.

With different parameters such as frequency f, θ_0, and r, and current **J** distributions, we recover the microwave images as shown in the following sections.

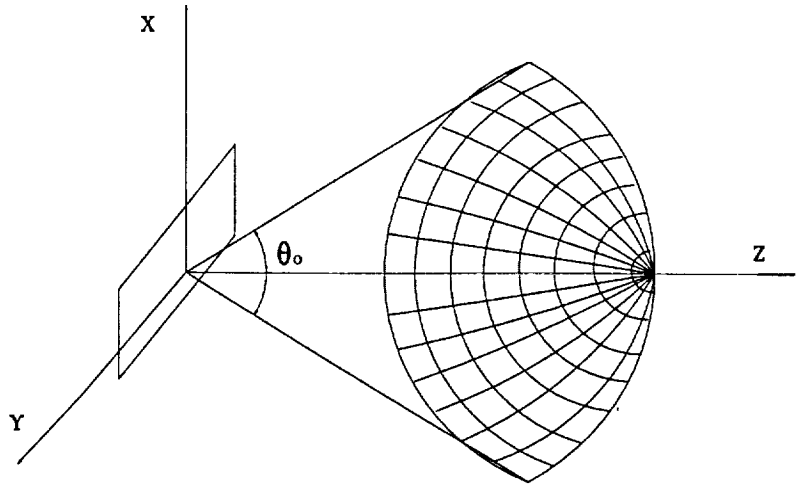

Figure 2.1 Spherical cap receiving surface

1) Simulation at Different Frequency

In these section, the original current **J** distribution is $|\mathbf{J}| = 1$ at the center element, and $|\mathbf{J}| = 0$ with others. The original current plane is still divided into 9×9 elements with area $S_J = 0.1\text{m} \times 0.1\text{m}$ of each element. The radius r of the sphere cap equals to 1λ. There are 54 measuring points on the receiving surface with the same r, different φ, and different θ (for spherical coordinate system) . ($\theta_0 = \frac{\pi}{2}$)

As you can see, when the frequency is lower than 0.11GHz, the amplitude of the images are very low, but you can get the outlook of the object through the images. When the f goes high, the amplitudes of the center point and around all increase. You can hardly tell what the original object is like comparing with other **J** distributions (Figure 2.3).

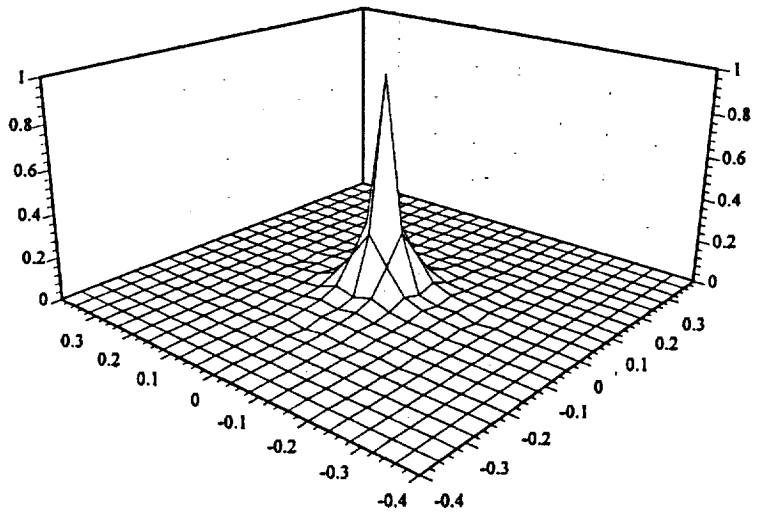

Figure 2.2 (a) The original current **J** with one-point distribution
9×9 square elements in **J** plane
54 elements in **E** surface

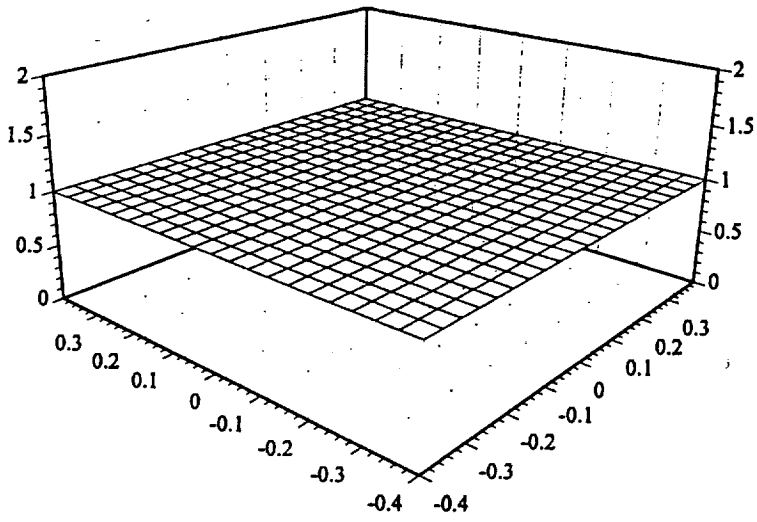

(b) Guessed **J** distribution

Figure 2.2 Continued

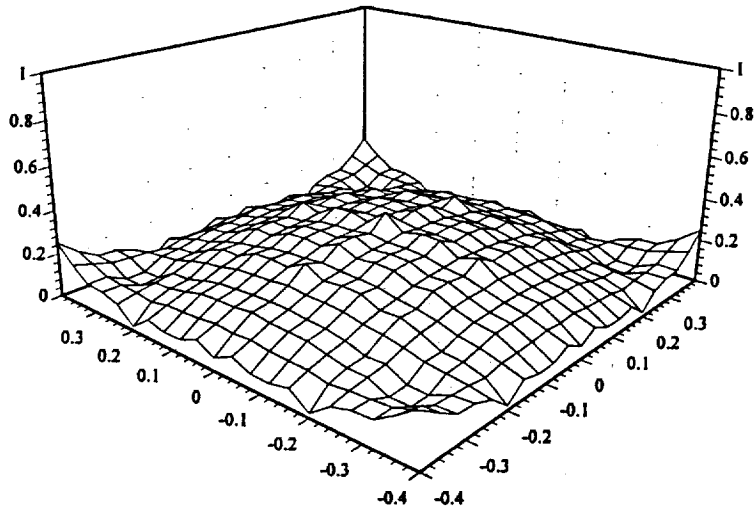

(c) Current image with f = 0.01GHz, r = 1λ

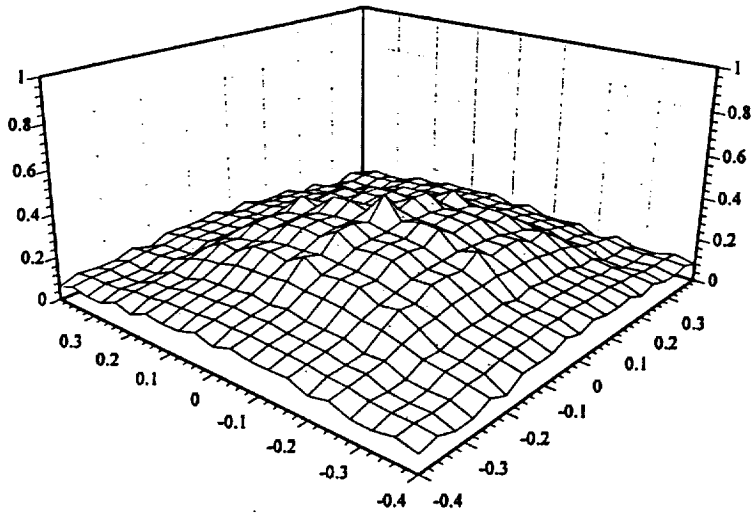

(d) Current image with f = 0.025GHz, r = 1λ

Figure 2.2 Continued

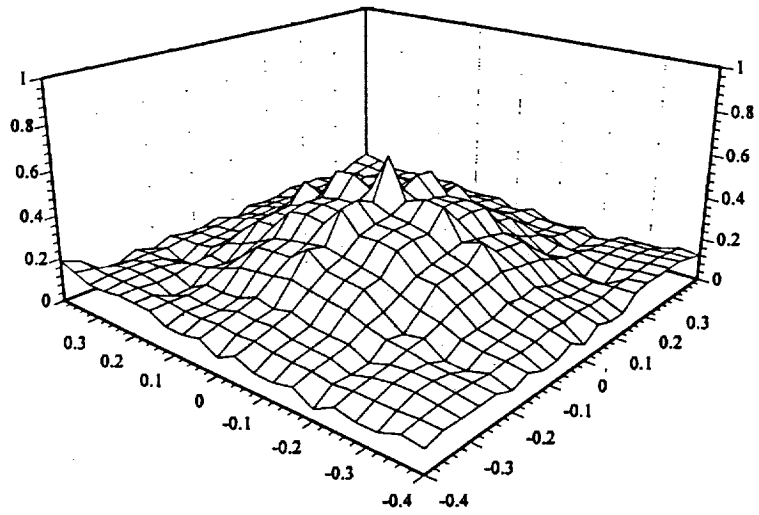

(e) Current image with f = 0.05GHz, r = 1λ

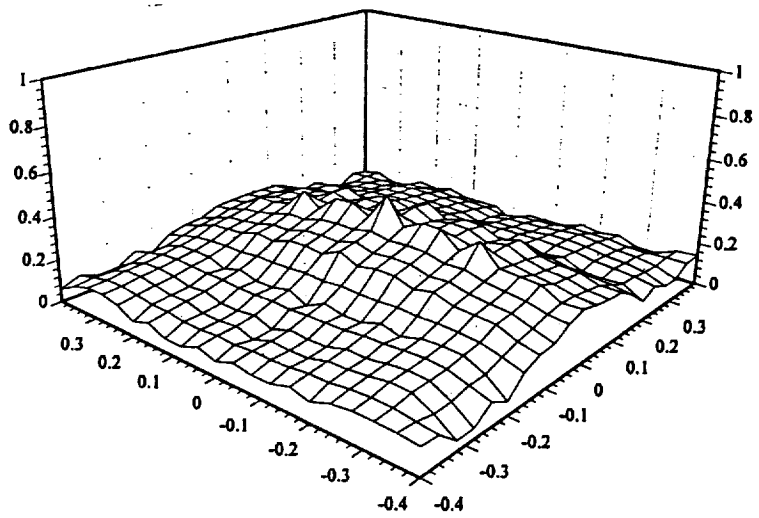

(f) Current image with f = 0.08GHz, r = 1λ

Figure 2.2 Continued

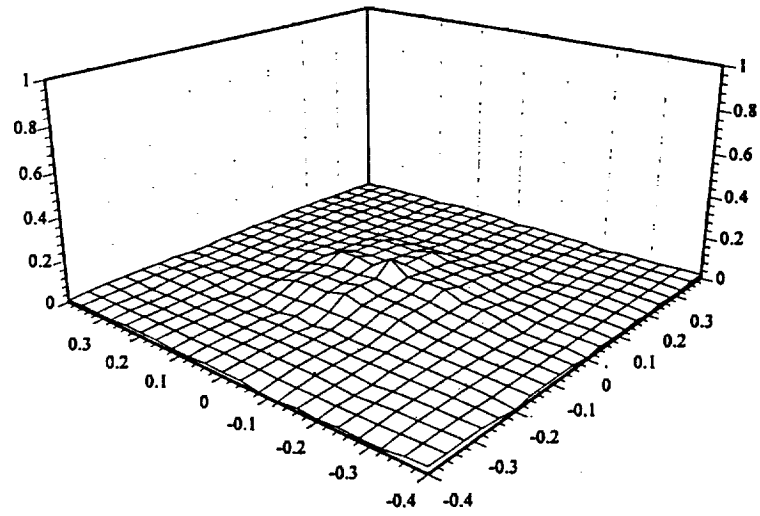

(g) Current image with f = 0.1GHz, r = 1λ

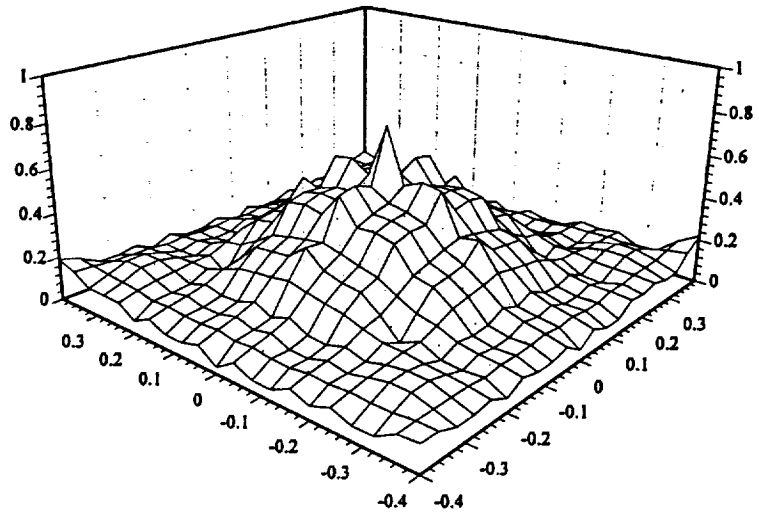

(h) Current image with f = 0.11GHz, r = 1λ

Figure 2.2 Continued

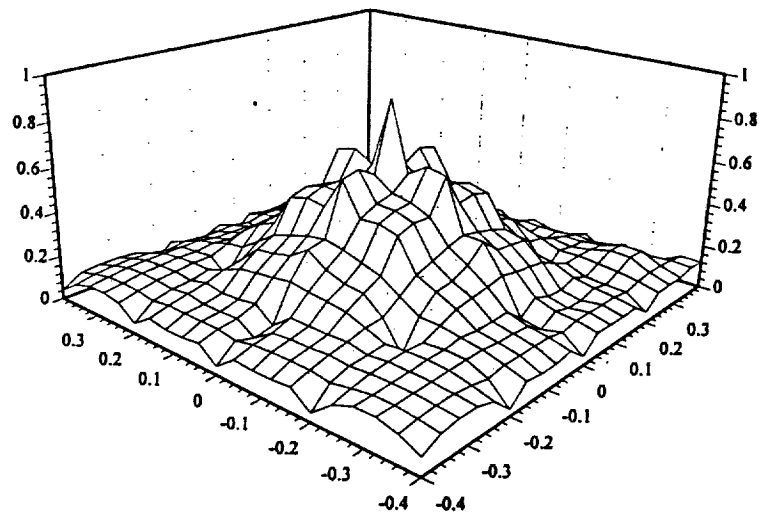

(i) Current image with f = 0.15GHz, r = 1λ

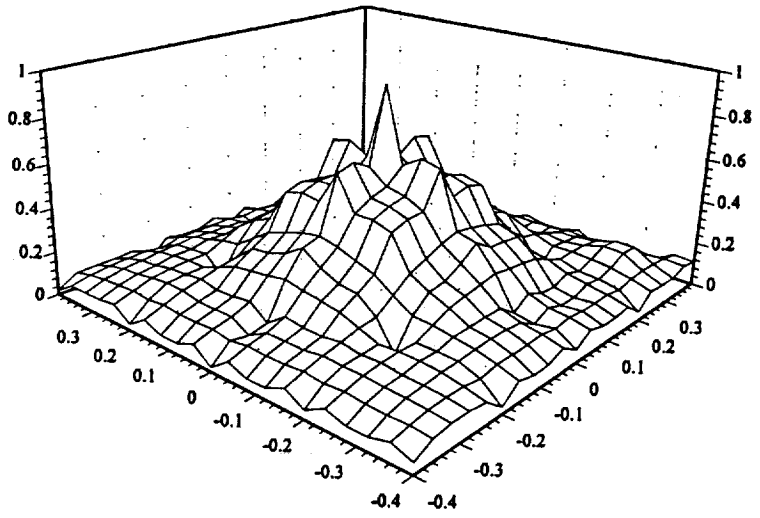

(j) Current image with f = 0.2GHz, r = 1λ

Figure 2.2 Continued

2) Simulation with Different θ_0

With different θ_0, the receiving elements vary much. When $\theta_0 = \frac{\pi}{2}$, the receiving surface is a hemisphere. As the θ_0 becomes small, this surface becomes a spherical cap. In this section, we will simulate with different θ_0. The original current **J** distribution is $|\mathbf{J}| = 1$ at the center 9 elements, and $|\mathbf{J}| = 0$ with others. The original current plane is still divided into 9×9 elements with area $S_j = 0.1\text{m} \times 0.1\text{m}$ of each element. The radius r of the sphere equals to 1λ. There are 54 measuring points on the receiving surface with the same r, different φ, and different θ (for spherical coordinate system) .

We can see that when $\theta_0 = \frac{\pi}{3}$, the image is better than anyone else.

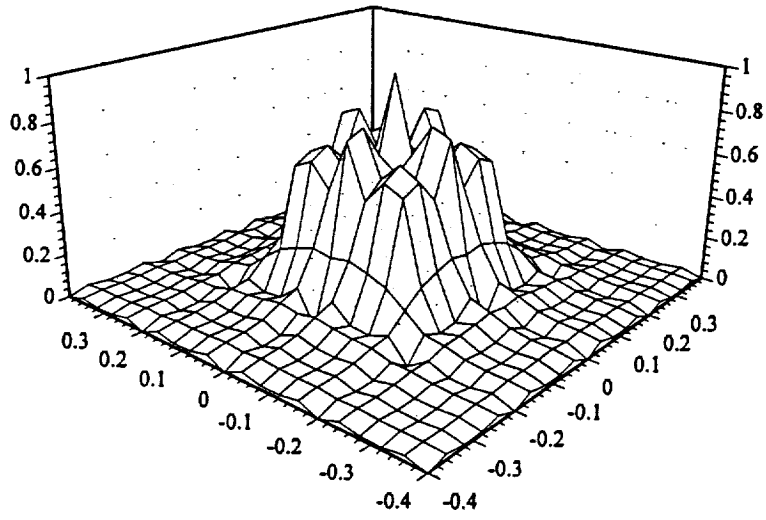

Figure 2.3 (a) The original current **J** with rectangular distribution
With f = 0.1GHz, r = 1λ
9 × 9 square elements in J plane
54 elements in E surface

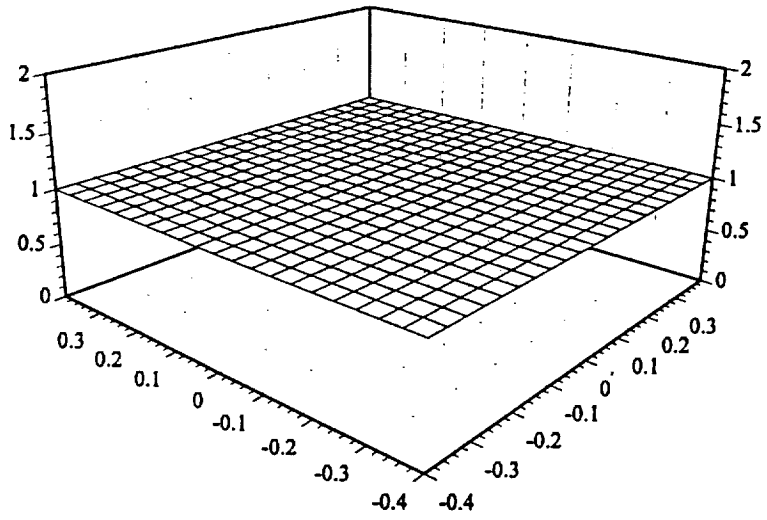

(b) Guessed **J** distribution

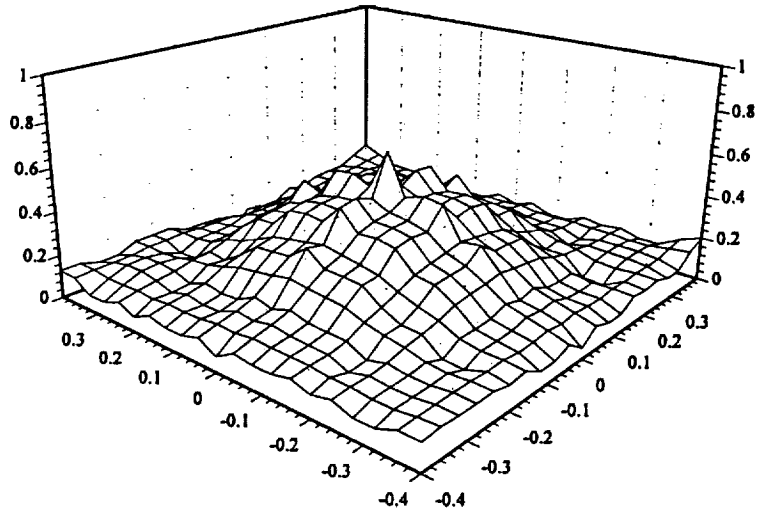

(c) Current image with $\theta_0 = \pi/6$

Figure 2.3 Continued

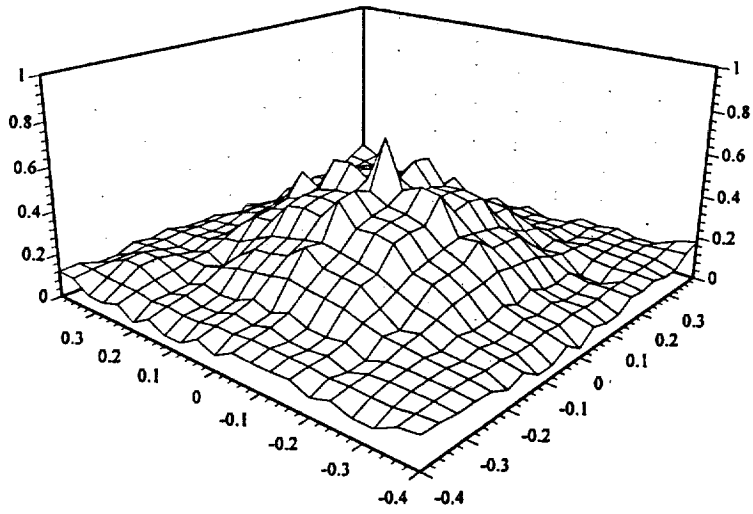

(d) Current image with $\theta_0 = \pi/5$

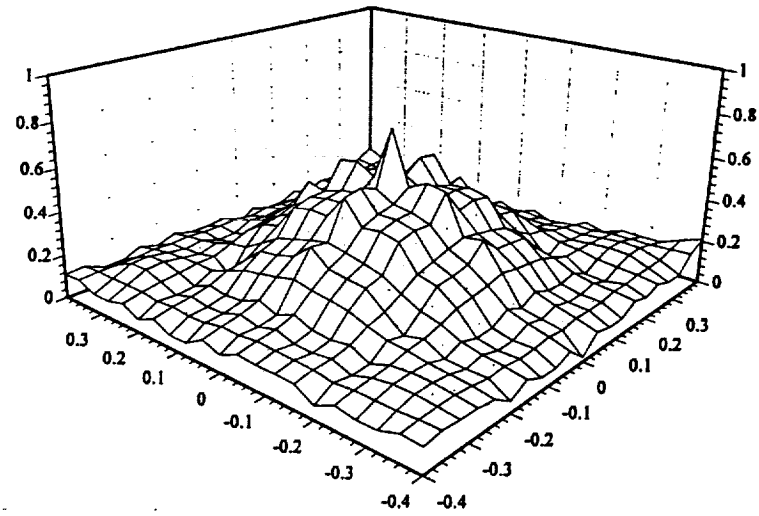

(e) Current image with $\theta_0 = \pi/4$

Figure 2.3 Continued

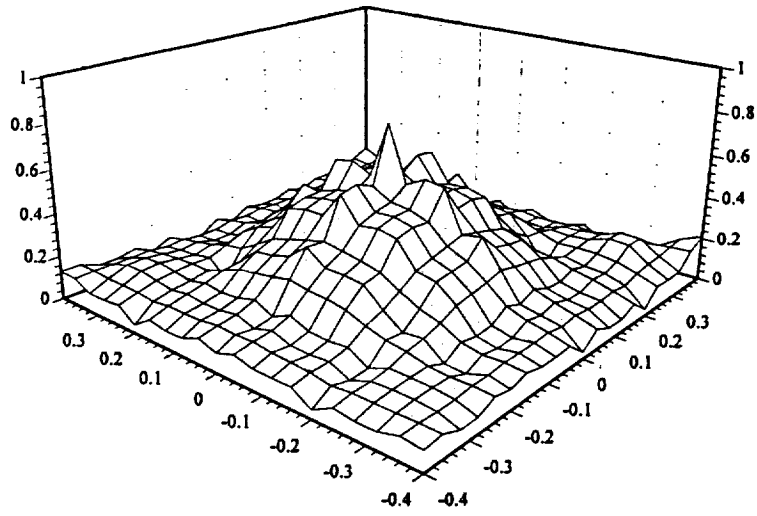

(f) Current image with $\theta_0 = \pi/3$

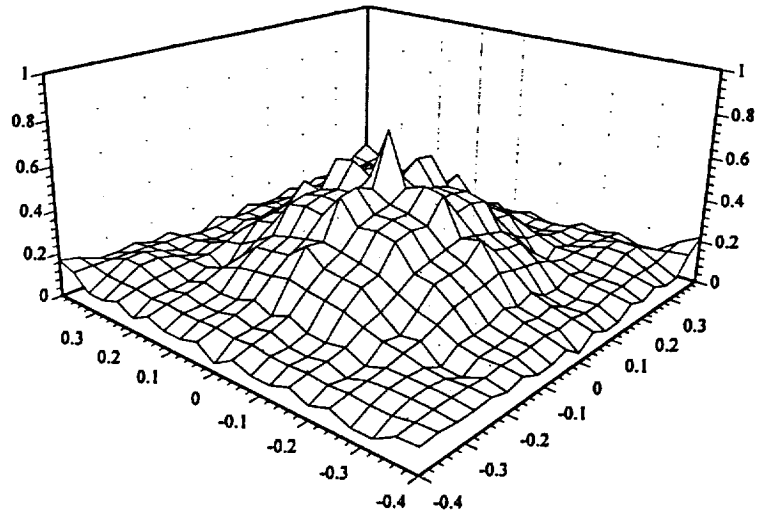

(g) Current image with $\theta_0 = 5\pi/12$

Figure 2.3 Continued

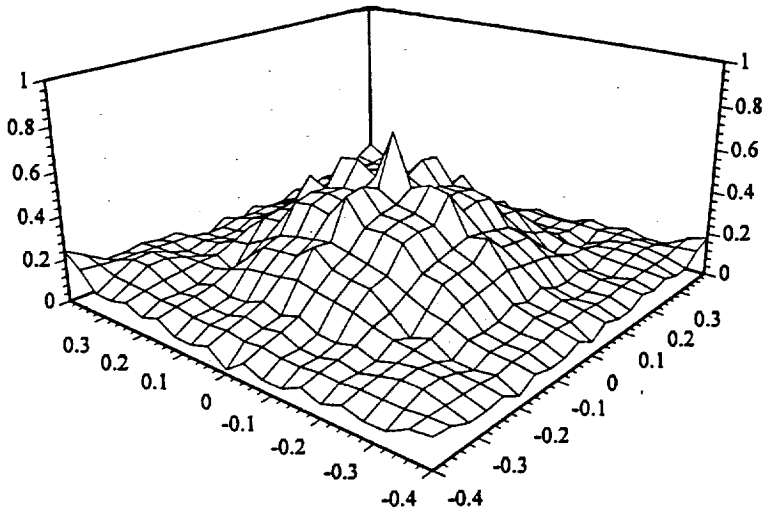

(h) Current image with $\theta_0 = \pi/2$

Figure 2.3 Continue

3) Simulation with Different r

Different radius r of the sphere cap receiving surface determines which field is measured: far field or near field. In this section, we will study the relation of radius r and the image recovered. The original current **J** distribution is $|\mathbf{J}| = 1$ at the central 9 elements, and $|\mathbf{J}| = 0$ with others. The original current plane is still divided into 9×9 elements with area $S_J = 0.1\text{m} \times 0.1\text{m}$ of each element. There are 54 measuring points on the receiving surface with different φ and different θ (for spherical coordinate system) . The radius r of the sphere cap varies and $\theta_0 = \frac{\pi}{2}$.

Increasing r, the amplitudes of the image decrease. When $r < 1\lambda$, the amplitudes decrease more than that when $r > 1\lambda$.

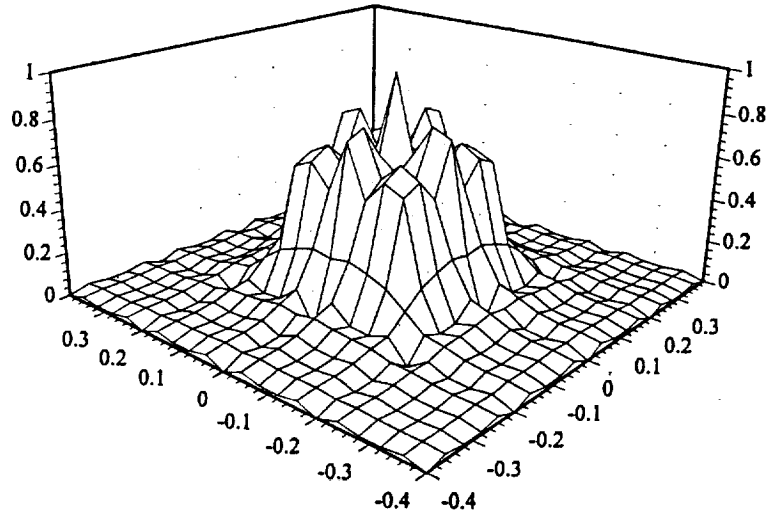

Figure 2.4 (a) The original current **J** with rectangular distribution

With f = 0.1GHz, $\theta_0 = \frac{\pi}{2}$

9 × 9 square elements in **J** plane

54 elements in **E** surface

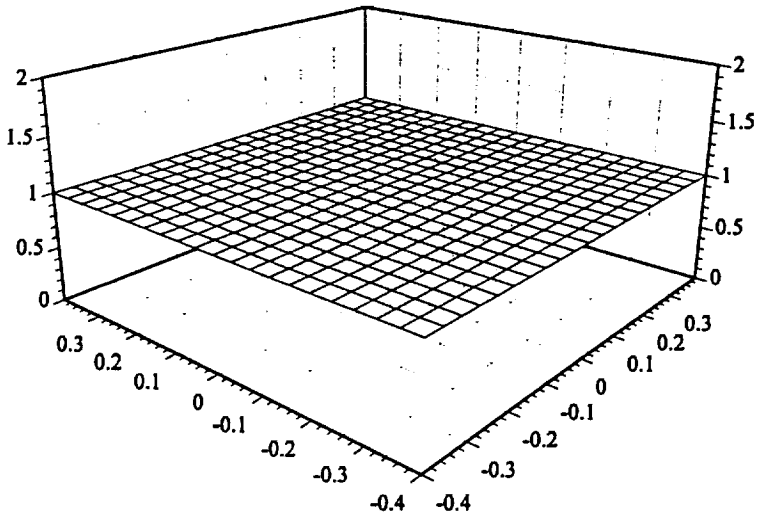

(b) Guessed **J** distribution

Figure 2.4 Continued

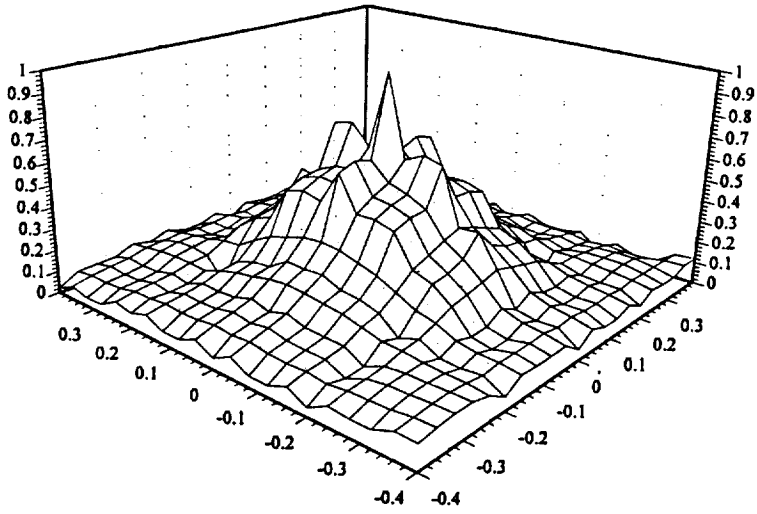

(c) Current image with $r = 0.4\lambda$

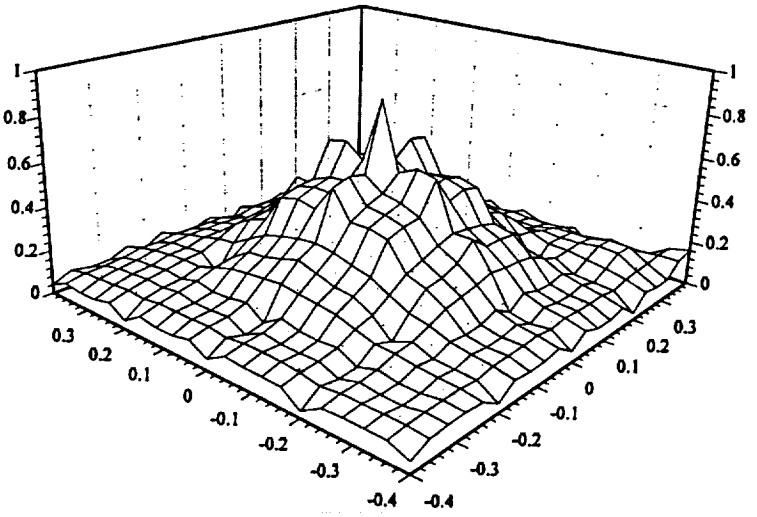

(d) Current image with $r = 0.6\lambda$

Figure 2.4 Continued

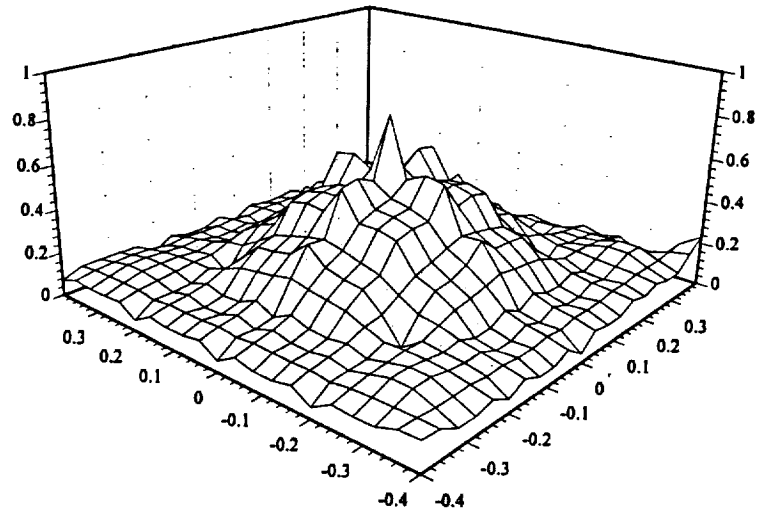

(e) Current image with $r = 0.8\lambda$

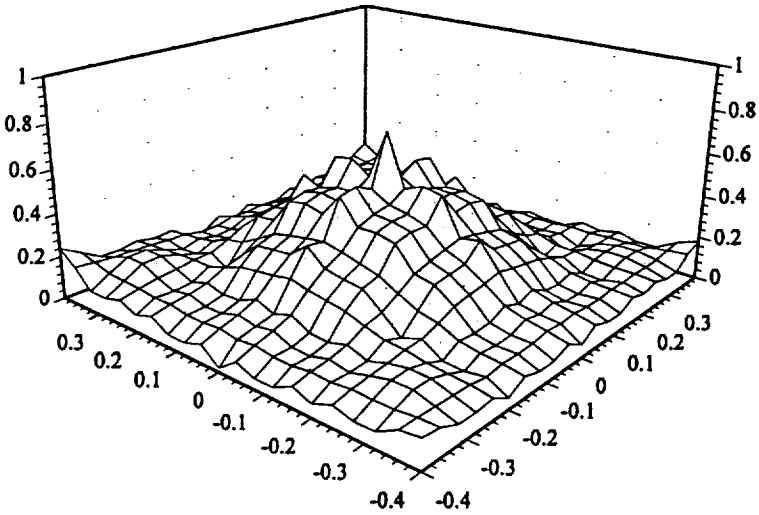

(e) Current image with $r = 1.0\lambda$

Figure 2.4 Continued

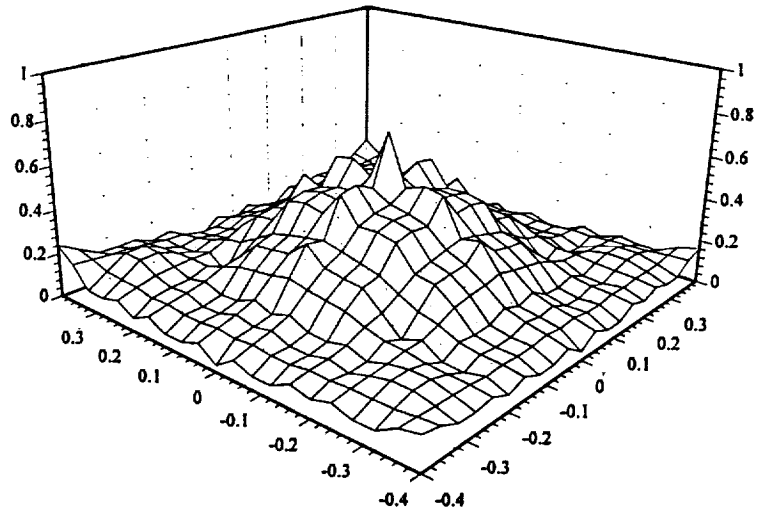

(f) Current image with $r = 1.2\lambda$

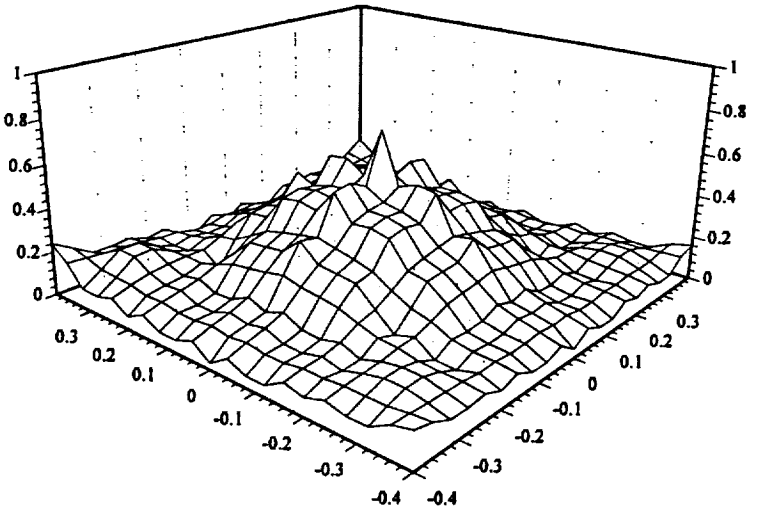

(g) Current image with $r = 1.4\lambda$

Figure 2.4 Continued

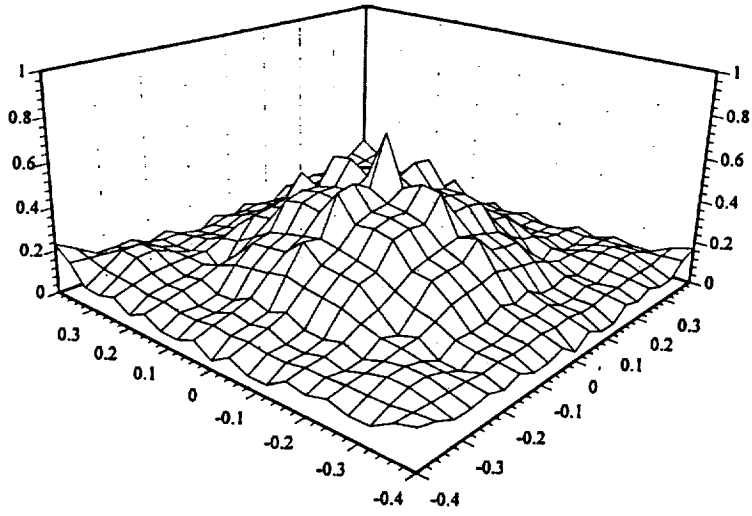

(h) Current image with $r = 1.6\lambda$

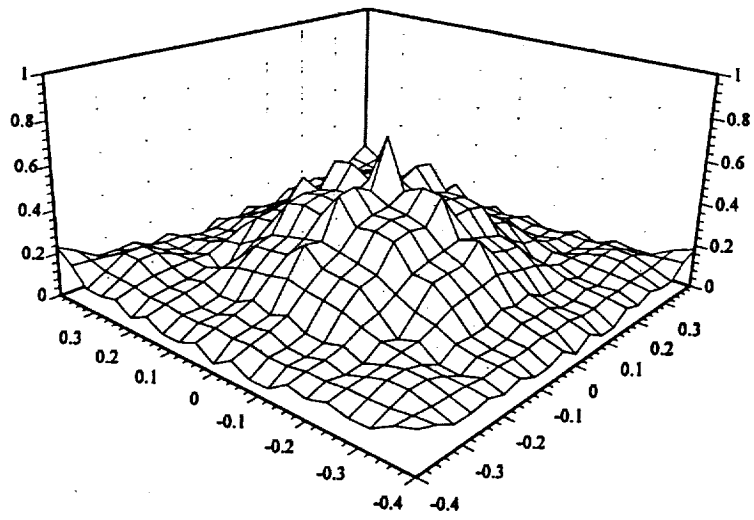

(i) Current image with $r = 1.8\lambda$

Figure 2.4 Continued

4) Simulation with Different Original Induced Current Distributions

In this section, we recover the microwave image with different original induced current **J** distribution. The original current plane is still divided into 9 × 9 elements with area $S_j = 0.1\text{m} \times 0.1\text{m}$ of each element. There are 54 measuring points on the receiving surface with different φ and different θ (for spherical coordinate system) . The radius r of the sphere equals to 1λ with $\theta_0 = \frac{\pi}{2}$ and $f = 0.1\text{GHz}$. In this section, the guess current distribution is the same in all the simulation as Figure 2.5 (b).

We can see that when the original plane contain more points whose amplitudes are not zero, it is easier to reconstruct the image than those have more zero amplitudes.

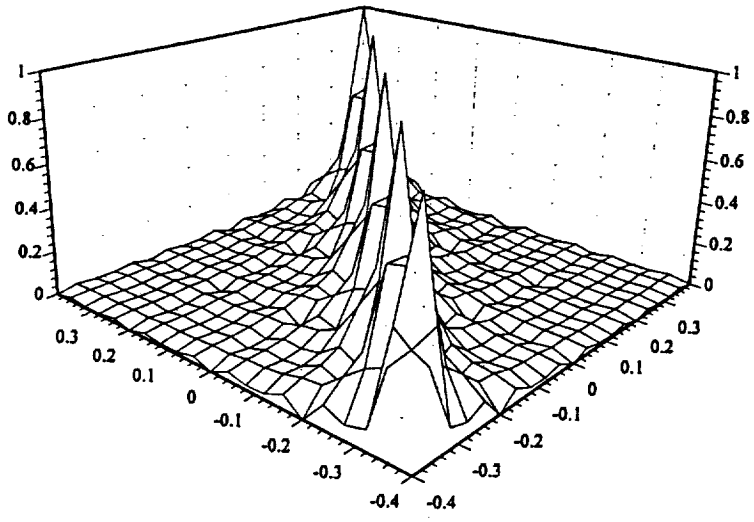

Figure 2.5 (a) The original current **J** with diagonal distribution
9 × 9 square elements in **J** plane
54 elements in **E** surface

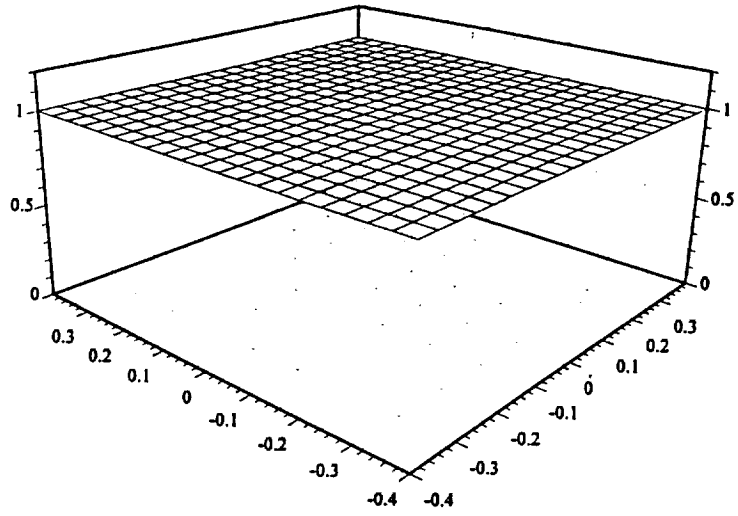

(b) Guessed **J** distribution

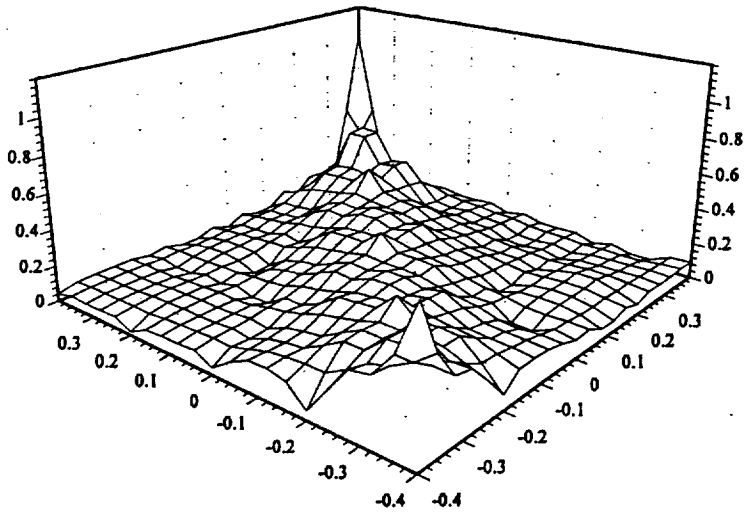

(c) Current image

Figure 2.5 Continued

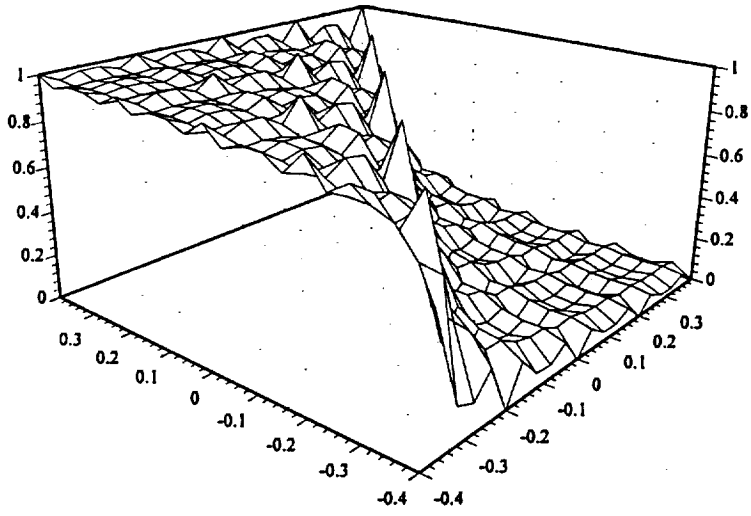

Figure 2.6 (a) The original current **J** with triangular distribution
9×9 square elements in **J** plane
54 elements in **E** surface

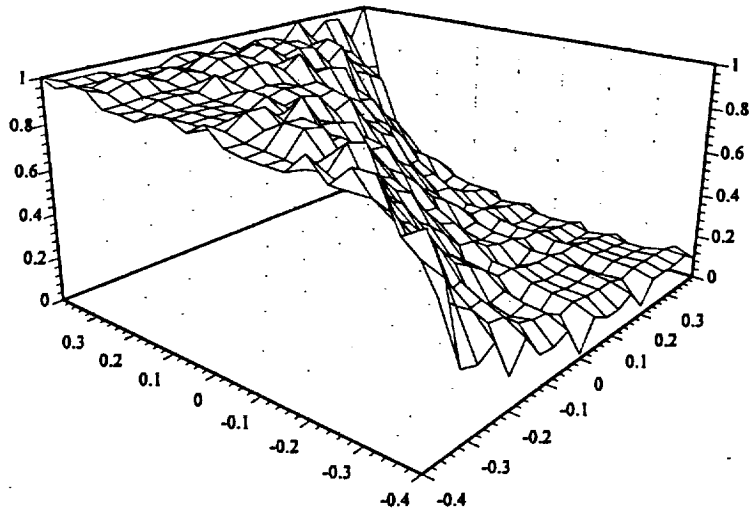

(b) Current image

Figure 2.6 Continued

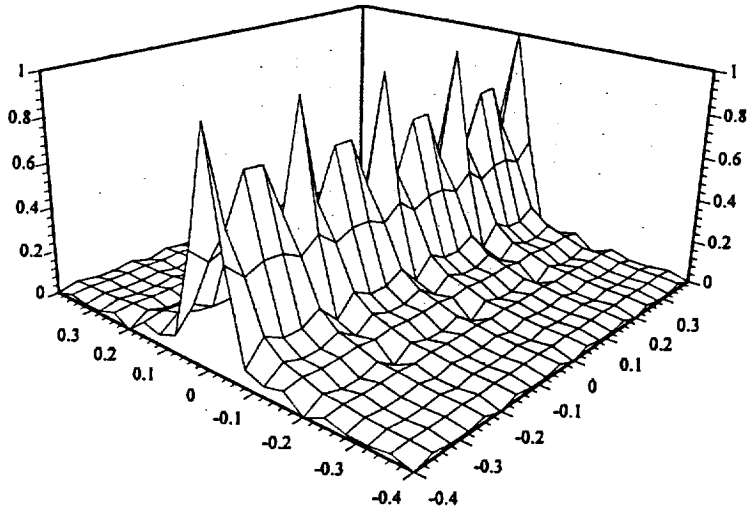

Figure 2.7 (a) The original current **J** with central line distribution
9×9 square elements in **J** plane
54 elements in **E** surface

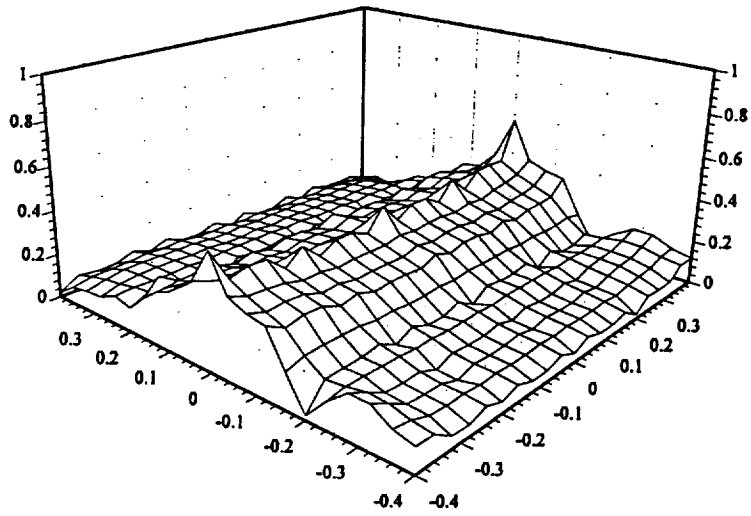

(b) Current image

Figure 2.7 Continued

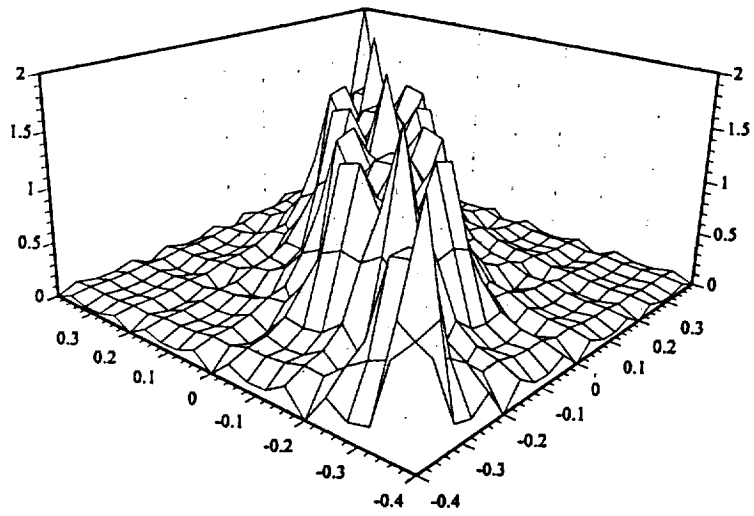

Figure 2.8 (a) The original current **J** with band diagonal distribution
9×9 square elements in **J** plane
54 elements in **E** surface

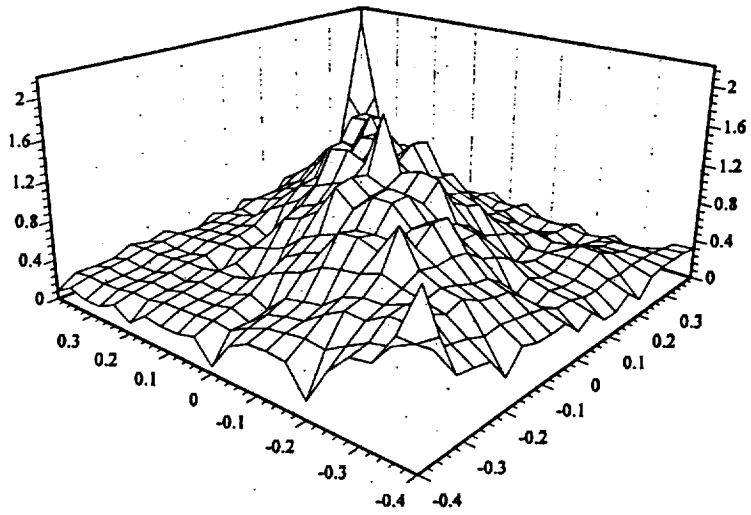

(b) Current image

Figure 2.8 Continued

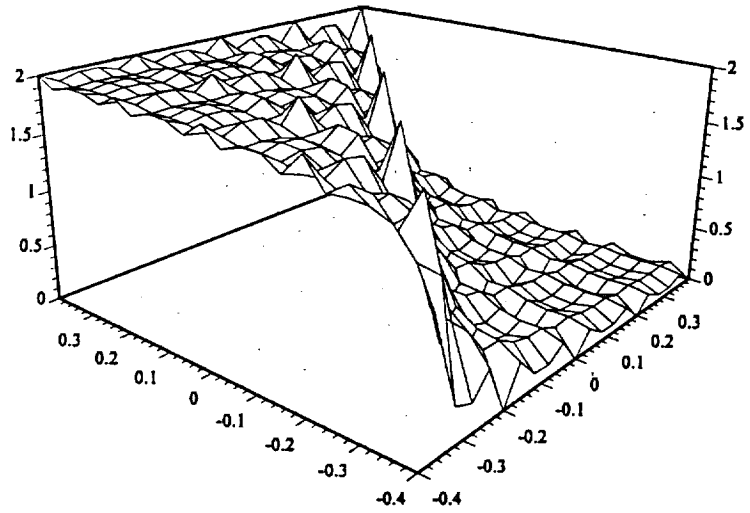

Figure 2.9 (a) The original current **J** with triagular distribution
9×9 square elements in **J** plane
54 elements in **E** surface

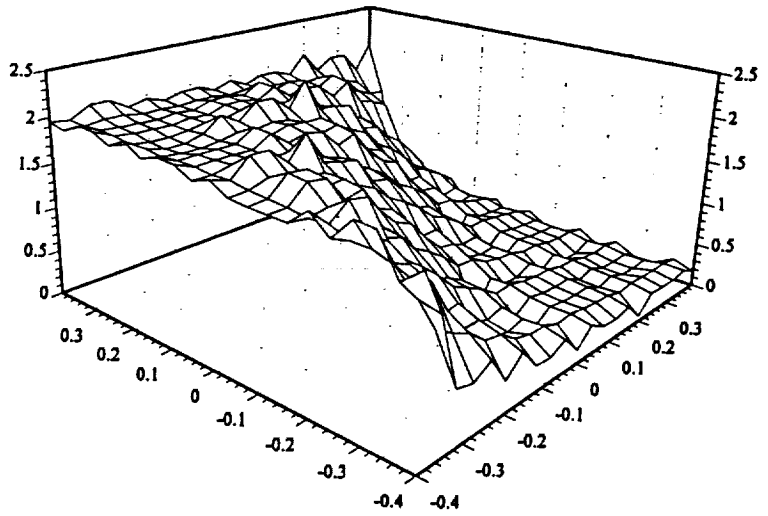

(b) Current image

Figure 2.9 Continued

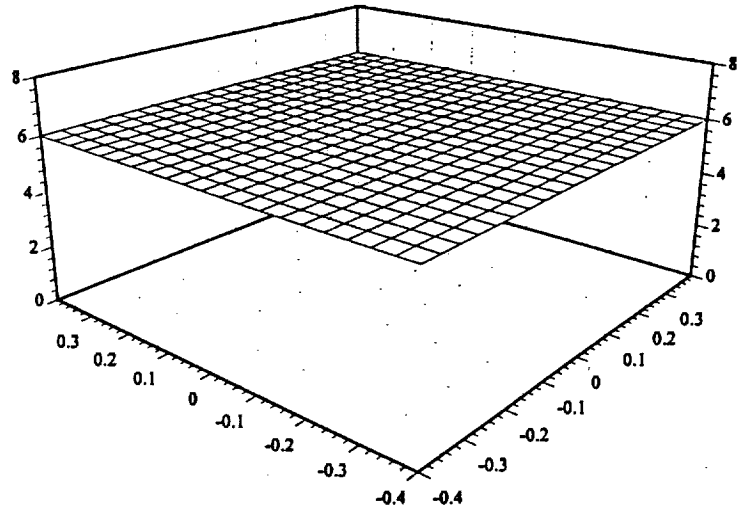

Figure 2.10 (a) The original current **J** with uniform distribution
9×9 square elements in **J** plane
54 elements in **E** surface

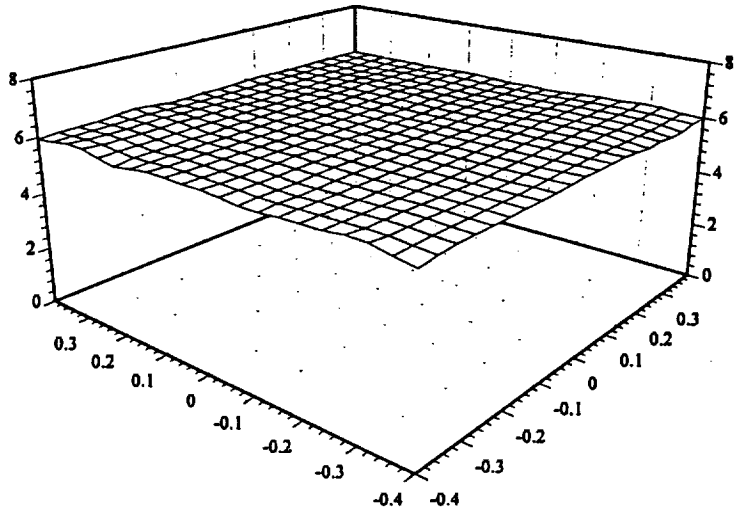

(b) Current image

Figure 2.10 Continued

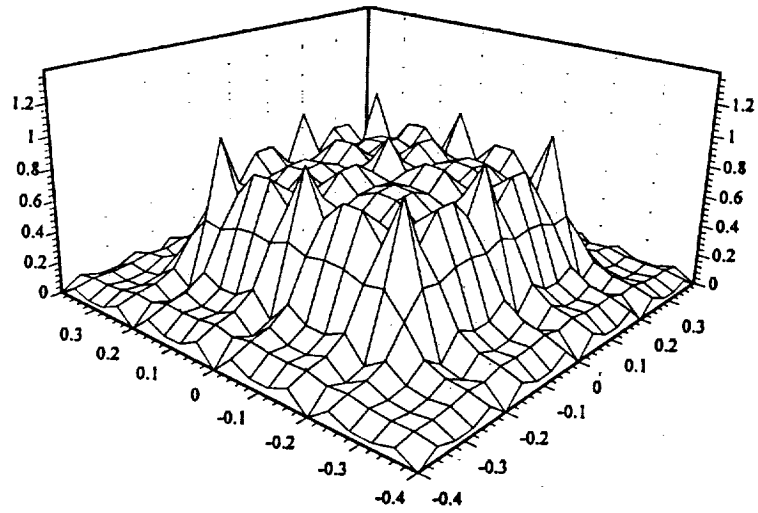

Figure 2.11 (a) The original current **J** with rectangular distribution
9×9 square elements in **J** plane
54 elements in **E** surface

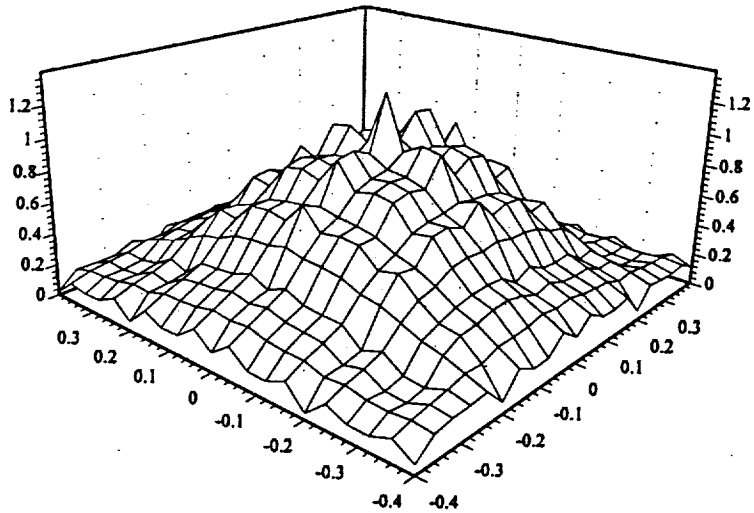

(b) Current image

Figure 2.11 Continued